Friction **11**(6): 1014–1026 (2023)
https://doi.org/10.1007/s40544-022-0642-5
ISSN 2223-7690
CN 10-1237/TH
RESEARCH ARTICLE

Efficacy of hierarchical pore structure in enhancing the tribological and recyclable smart lubrication performance of porous polyimide

Hongwei RUAN[1,2], Yaoming ZHANG[1], Fuzhi SONG[1], Qihua WANG[1,2], Chao WANG[1,*], Tingmei WANG[1,2,*]

[1] *Key Laboratory of Science and Technology on Wear and Protection of Materials, Lanzhou Institute of Chemical Physics, Chinese Academy of Sciences, Lanzhou 730000, China*

[2] *Center of Materials Science and Optoelectronics Engineering, University of Chinese Academy of Sciences, Beijing 100049, China*

Received: 10 November 2021 / Revised: 26 January 2022 / Accepted: 25 April 2022

© The author(s) 2022.

Abstract: Herein, a porous oil-containing material with hierarchical pore structure was successfully prepared through microtexturing large pores on the surface of porous polyimide (PPI) with single-level small pores. Compared to the conventional oil-containing material, the hierarchically porous oil-containing material exhibited high oil-content, and retained excellent mechanical properties and high oil-retention because of the synergistic effects of large pores and small pores. Furthermore, the lubricant stored in the hierarchically porous polyimide could release to the interface under thermal-and-mechano-stimuli, and the released lubricant could be reabsorbed into the hierarchically porous polyimide via the capillary-force offered by the porous channel. Based on the high oil-content and recyclable oil release/reabsorption, the hierarchically porous oil-containing polyimide exhibited excellent lubrication performance (coefficient of friction was 0.057). Furthermore, the composite could perform 1,069 cycles of smart lubrication (1 h per cycle), which significantly extended the service life of the hierarchically porous oil-containing smart lubrication material.

Keywords: recyclable smart lubrication; hierarchical pore structure; oil-content and oil-retention; friction and wear

1 Introduction

Lubrication is the most effective way to reduce friction and wear [1–4]. Solid lubrication (SL) and external oil supply lubrication (EOL) are commonly used lubrication methods. SL refers to the use of solid powders or films to reduce friction and wear and protect surface from damage [5–7]. However, the high coefficient of friction (COF), inevitable abrasion, the difficulty of discharging wear debris, and large vibration of SL (such as graphite, molybdenum disulfide, and Polytetrafluoroethylene (PTFE)) limit their application in high-precision and long-life motion components [8–10]. Instead, the EOL boost lubrication equipment and lubricant consumption [11]. Smart lubrication offers a possible solution to reduce the shortcomings of SL and EOL through responding to external stimuli and achieving lubrication performance [12]. Porous oil-containing material that is generated through lubricant imbibition into the pore structure of matrix is a typical recyclable smart lubrication material, which can realize lubrication through continuous oil release in feedback to external stimuli and oil reabsorption induced via capillary- force provided by the matrix [13–16].

Due to the load-bearing and oil storage properties of the matrix, the pore structure of matrix is vitally important for porous oil-containing material. At present, the pore structure of porous oil-containing material is prepared by introducing porous filler into the matrix [13, 17], microtexturing the pore structure on

* Corresponding authors: Chao WANG, E-mail: wangc@licp.cas.cn; Tingmei WANG, E-mail: tmwang@licp.cas.cn

the surface of substrate (such as polymer and metal) [18, 19], and self-forming three-dimensional coherent porous network in the matrix [20–22]. However, the porous fillers introduced into the polymer matrix are difficult to uniformly disperse, which may cause the porous fillers to be enclosed in the matrix and prevent the lubricant from storing and supplying. For microtexturing the pore structure on the surface of the matrix, only a small amount of lubricant can be stored, which seriously reduces the service life of the material. Since the lubricant cannot be continuously release, the porous oil-containing materials will undergo vibration, noise, and size changes, resulting in a series of mechanical failures. The oil-content is an important parameter that determines the life of porous oil-containing smart lubrication materials [23]. Therefore, self-forming a three-dimensional coherent porous network in the matrix is a common method for porous oil-containing smart lubrication materials, which can store more lubricant and release lubricant under thermal-and-mechano-stimuli to achieve lubrication. Moreover, the released lubricant can be reabsorbed into the porous matrix by capillary-force provided by the channel of the porous matrix.

Conventionally, research on porous oil-containing smart lubrication materials with three-dimensional porous network has focused on forming porous matrix with large pores or high porosity to store more lubricant to obtain low COF. For example, Wang's group [24–26] developed a series of porous polymer matrices with large pores through templating methods (sodium chloride as a template) to store more lubricant and obtain a low COF. Nevertheless, the large pore size was accompanied by low oil-retention, which caused more lubricant to leak and shortened the service life of porous oil-containing material. A self-forming three-dimensional coherent porous matrix with high porosity has been suggested to be promising in storing more lubricant and obtaining high oil-retention but cannot retain mechanical strength [16, 23]. Porous oil-containing smart lubricating materials with high oil storage properties (oil content and oil retention) and mechanical strength at the same time have proven to challenging. Hierarchically porous materials, which possess large and small pores in the matrix, show great potential for lubricant storage owing to their large accessible space and excellent accommodation capability with volume [27–30]. In addition, the hierarchically porous material could retain the mechanical strength and oil-retention because of the synergistic effects of large and small pores.

Herein, we developed a hierarchically porous oil-containing material through lubricant imbibition into a hierarchically porous matrix. The small pores of hierarchically porous matrix played role of retaining the mechanical strength and high oil-retention, and the large pores played role of improving the oil-content. Because of the synergistic effects of the large pores and small pores, hierarchically porous oil-containing material significantly increase the oil-content (the oil-content of porous polyimide (PPI) was 12.01%, and the oil-content of HPPI was 20.85%), enhance the tribological performance (COF was 0.057), and achieve recyclable lubricant releasing/reabsorbing. The present study is expected to pave the way for the development of novel oil-containing materials.

2 Experimental

2.1 Materials

Thermoplastic polyimide (YS-20) powder and polyalphaolefin 10 (PAO 10) were sourced from Shanghai Synthetic Resin Institute (China) and ExxonMobil Chemical Co. Ltd., respectively. Ethanol, acetone, and petroleum ether were obtained from Sinopharm Chemical Reagent Co. Ltd. (China). All chemicals were used as received without further purification.

2.2 Preparation of hierarchically porous oil-containing polyimide

The PPI with single-level small pores was fabricated by cold pressing and hot sintering process, and the porous polyimide with a hierarchically coherent pore structure (HPPI) was fabricated through microtexturing large pores on the surface of PPI [31], and nonporous polyimide (PI) was fabricated by hot pressing of polyimide powder. To satisfy the tribological test and surface microtexturing, the PPI and PI were cut into 18 mm × 18 mm × 2 mm squares. HPPI was prepared through microtexturing large pores on the surface of the PPI. All the center distances of the large pores were 200 μm, and the pore diameters were 50, 100, and 150 μm, marked as HPPI-T50, HPPI-T100, and

HPPI-T150, respectively. The depth of the large pores was approximately 90 μm (HPPI- T50: 91.1 μm, HPPI-T100: 106.7 μm, HPPI-T150: 83.4 μm). As a control, PI textured large pores of 100 μm (PI-100). All the samples were washed sequentially in ethanol, acetone, and petroleum ether solutions for 24 h, and then the sample was removed and placed in an oven at 120 °C to dry for 24 h under a vacuum environment. After drying, PPI, PI-100, HPPI-T50, HPPI-T100, and HPPI-T150 were immersed in PAO10 in a vacuum oven at 120 °C for 24 h and then cooled to room temperature. The sample was removed, and the lubricant on the surface was wiped off with a cotton cloth. The oil-containing PPI, PI-100, HPPI-T50, HPPI-T100, and HPPI-T150 were marked as OCPPI, OCPI-100, OCHPPI-T50, OCHPPI-T100, and OCHPPI-T150, respectively.

2.3 Characterization

The pore size and porosity of the PPI were tested by mercury porosimetry (Micromeritics Autopore9500, USA). The cross-sectional and surface topography of HPPI were tested by field emission scanning electron microscope (SEM, Mira 3, Xmu, Tescan). According to GB1041, the mechanical performances were analyzed by an electron omnipotence experiment machine SANS-CMT5105 (China) under ambient conditions. The sample size was 10 mm × 10 mm × 4 mm, the stress at 25% deformation was taken as the compressive strength, and the elastic modulus was calculated by the slope of the elastic deformation zone.

The oil-content was calculated according to Eq. (1), and the oil-retention was calculated by Eq. (2). The oil-retention performance of oil-containing sample was tested by a high-speed centrifuge under 3,000 rpm. In addition, the minimum centrifugal speed that the lubricant can release was calculated by Laplace's load–Darcy's law, as shown in Eq. (3).

$$\text{Oil-contain} = \frac{m_1 - m_0}{m_0} \times 100\% \tag{1}$$

$$\text{Oil-retention} = \frac{m_i - m_0}{m_1 - m_0} \times 100\% \tag{2}$$

$$\omega_C = 2\left[\frac{\gamma lv\varphi}{\rho R_{\text{pore}} r_0 (r_0 - r_i)}\right]^{\frac{1}{2}} \tag{3}$$

where m_0 is the mass of the dry sample; m_1 is the mass of the oil-containing sample; and m_i is the oil-containing sample after centrifugation for a period of time. φ is the porosity of the PPI, and γlv is the surface tension of the lubricant. ρ, R_{pore}, r_0, and r_i are the density of the porous matrix impregnated PAO10, the average pore radius of the oil-containing porous matrix, the outer radius, and the inner radius of the centrifuge except the diameter of the composite, respectively.

2.4 Tribology test

The tribological performance of all samples were tested on a universal mechanical tester (UMT-3, Bruker) in ball-on-disk contact mode. A GCr15 steel ball (diameter = 3 mm) was selected as the counterpart. The wear rate of all samples was calculated as follows:

$$\text{Wear rate} = \frac{V}{PL} \tag{4}$$

Here, V, P, and L are the amount of wear, applied load and sliding distance, respectively.

3 Results and discussion

3.1 Pore structure, mechanical strength, and oil storage performance

The pore structure on the surface and interior of the porous matrix is the basis for lubricant storage and release. Mercury porosimeter was used to obtain pore size and porosity in the studied porous matrix, and SEM was used to obtain morphology of the pore structure. The mercury in- out curve and pore size distribution are shown in Fig. 1. The mercury in-out curve in Fig. 1(a) indicates that the porosity of PPI is 19.2% [32]. The pore size distribution curve in Fig. 1(b) demonstrates that the pore size of PPI is approximately 0.92 μm. The mercury porosimeter results show that coherent porous structures were observed in PPI. Figure 2 displays the surface morphology of PPI, HPPI-T50, HPPI-T100, and HPPI-T150, showing that the sizes of the large pore on the surface are 50, 100, and 150 μm. Furthermore, Fig. 3 shows the cross- sectional morphology of PPI, HPPI-T50, HPPI-T100, and HPPI-T150, exhibiting that the depths of the large pore on the surface are

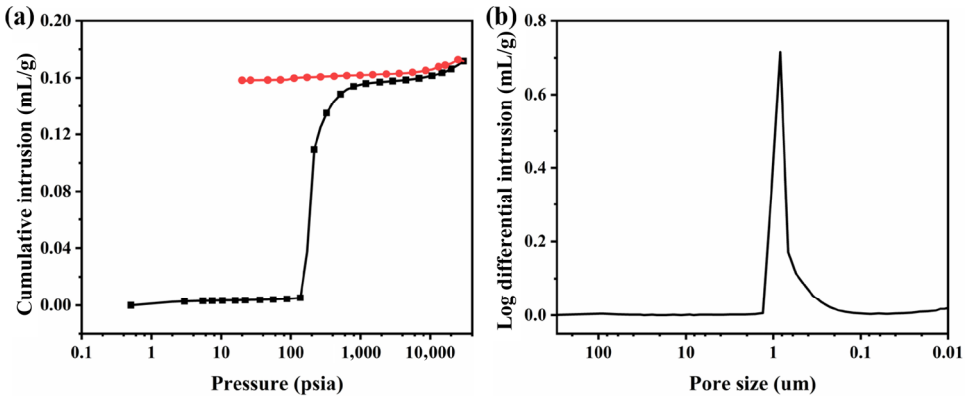

Fig. 1 (a) Mercury intrusion (black) and extrusion (red) curve, and (b) the pore size distribution of PPI based on mercury intrusion porosimetry.

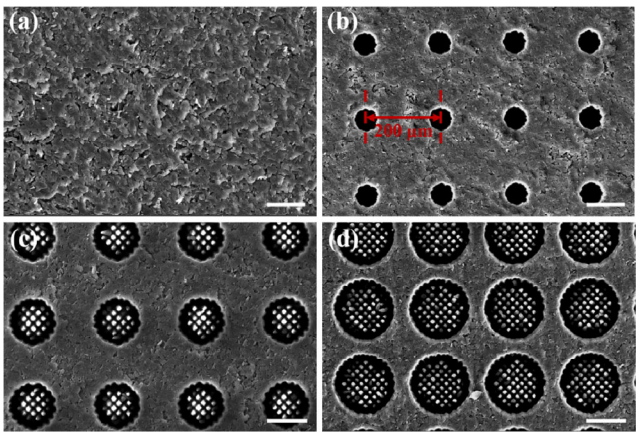

Fig. 2 (a) Surface morphology (scale bar: 100 μm) of PPI, (b) HPPI-T50, (c) HPPI-T100, and (d) HPPI-T150.

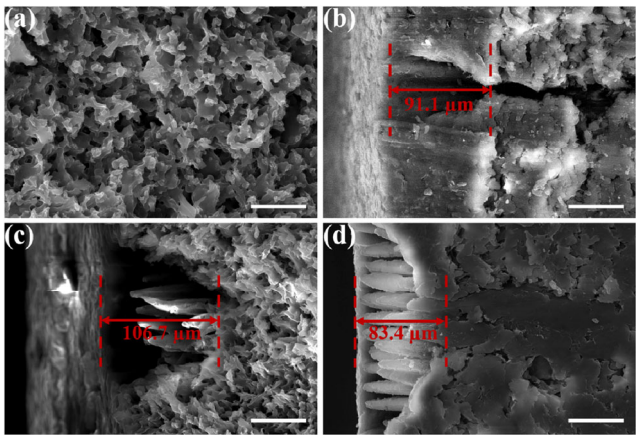

Fig. 3 Cross-sectional morphology (scale bar: 50 μm) of (a) PPI, (b) HPPI-T50, (c) HPPI-T100, and (d) HPPI-T150.

approximately 90 μm (HPPI-T50: 91.1 μm, HPPI-T100: 106.7 μm, HPPI-T150: 83.4 μm). The surface and cross-sectional morphology of porous matrices demonstrate not only that the hierarchical pore structures were successfully prepared but also that the large pores connected with the small pores. To retain high oil-retention, micropillars were prepared in the large pores of HPPI-T100 and HPPI-T150 by adjusting the laser spacing of microtexturing, which divided the large pores into numerous regions. The coherent hierarchical pore structure offers a solid foundation for high oil storage.

The oil-content and oil-retention of oil-containing samples are exhibited in Fig. 4. Compared with OCPPI (oil-content = 12.01%), the oil-content of OCHPPI-T50, OCHPPI-T100, and OCHPPI-T150 (Fig. 4(a)) increased by 2.01%, 6.19%, and 8.84%, respectively. Because the large pores were introduced on the surface of PPI, hierarchically porous polyimide could impregnate more lubricant into the porous matrix and significantly increase the oil-content. Simultaneously, the oil-retention performance was performed on a high-speed centrifuge at 3,000 rpm. When the centrifugal force was greater than the capillary-force provided by the channel of the porous matrix, the lubricant stored in pores was released. Compared with OCPPI (oil-retention = 81.8%), the oil-retention of OCHPPI-T50, OCHPPI-T100, and OCHPPI-T150 (Fig. 4(b)) decreased by 10.7%, 2.5%, and 6% with 120 min centrifugation, respectively. Because the capillary-force provided by the channel of the porous matrix decreases as the pore size increases, the porous matrix with a larger pore size leaks more lubricant when the centrifugation speed is the same. However, the oil-retention of OCHPPI-T100 and OCHPPI-T150 was greater than that of OCPPI-T50. This was attributed to the specific structure of micropillars stacked in the

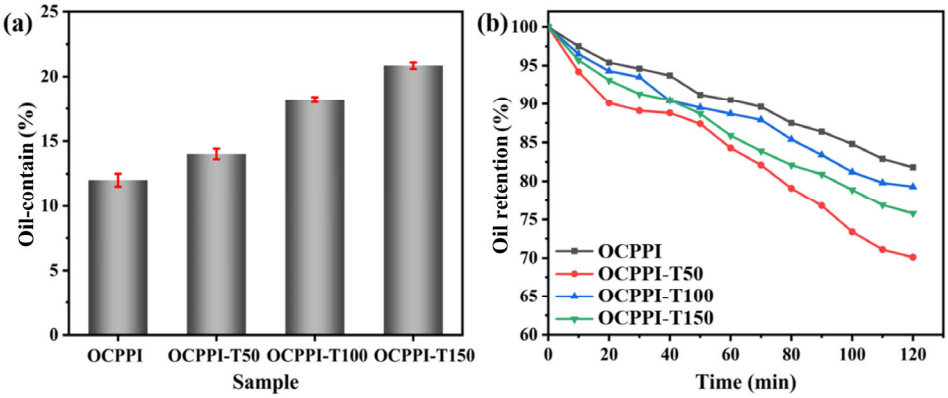

Fig. 4 Oil-content and oil-retention of different samples.

large pores, which facilitated the additional capillary-force between the micropillars, OCHPPI-T100, and OCHPPI-150 provided a higher oil-retention. The higher oil-retention indicates slow and stable oil release, significantly extending the service life of the material.

Mechanical properties are also important factors affecting tribological properties, and lower mechanical properties may lead to higher wear. The compressive strength and elastic modulus of different samples are shown Fig. 5. Compared with PPI, the compressive strength and elastic modulus of the HPPI (Fig. 5(a)) do not decrease significantly (the compressive strength of PPI was 130.1 MPa, and the compressive strength of HPPI-T150 is 127 MPa). At the same time, the elastic modulus (Fig. 5(b)) also did not decrease significantly. In this study, only the surfaces of PPI were processed, and the interior pore structure was not changed. Therefore, the mechanical strength of the hierarchically porous polyimide did not obviously decrease. The higher mechanical strength guarantees the lubrication performance of the porous oil-containing material.

3.2 Effect hierarchical pore structure on the tribological performance

In order to investigate the effect of the hierarchical pore structure on lubrication performance, the tribological properties of OCPPI, OCHPPI-T50, OCHPPI-T100, and OCHPPI-T150 were performed on a friction and wear testing machine under 10 N and 5 Hz, and the test lasted 150 min. The COF is shown in Fig. 6(a), and the results demonstrate that the COFs of OCPPI, OCHPPI-T50, OCHPPI-T100, and OCHPPI-T150 are 0.105, 0.094, 0.057, and 0.076, respectively. As the large pore size increased, the COF decreased by 10.48%, 45.71%, and 27.62%. The results demonstrate that introducing large pores on the surface of PPI could significantly reduce the COF, especially large pores with a diameter of 100 μm. In addition, to

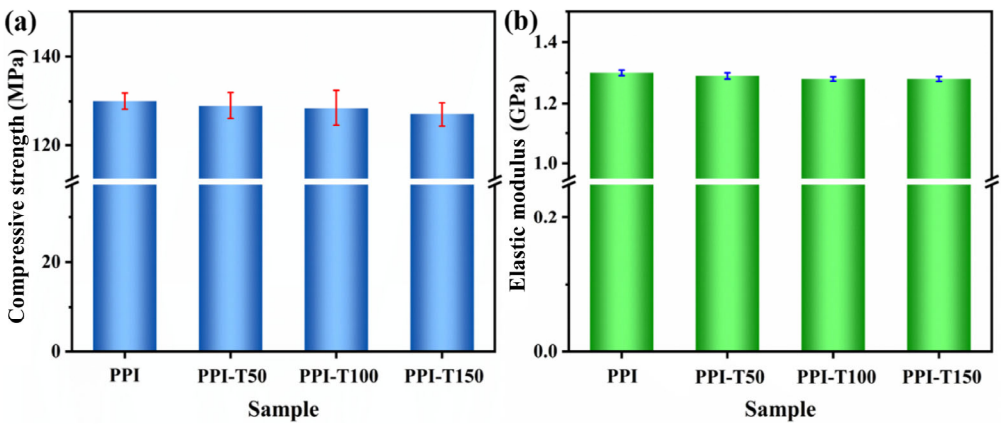

Fig. 5 (a) Compressive strength and (b) elastic modulus of different samples.

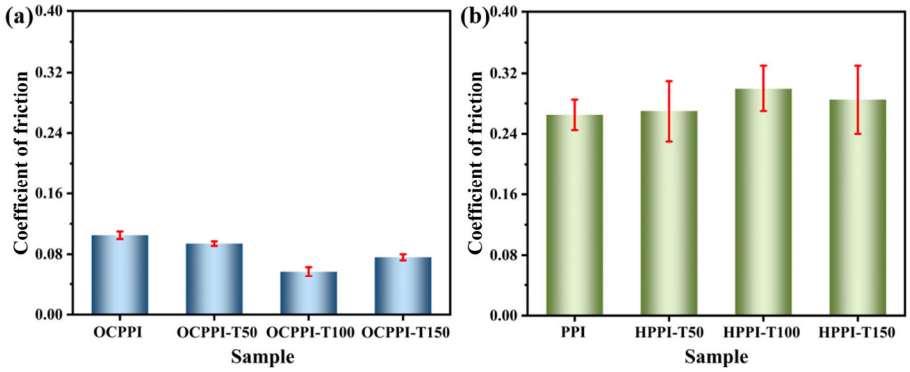

Fig. 6 COF of (a) oil-containing and (b) dry samples.

investigate the effect of lubricant on the tribological performance, the tribological performance of dry samples were tested under same conditions as oil-containing samples. The COF is shown in Fig. 6(b), and the results show that the COFs of dry PPI, dry HPPI-T50, dry HPPI-T100, and dry HPPI-T150 are 0.265, 0.27, 0.3, and 0.285, respectively. The large pores introduced on the surface of PPI caused the COF to increase. This was ascribed to the fact that larger shear force was generate by large pores.

To study the friction and wear mechanism, the surface morphology of OCPPI, OCHPPI-T50, OCHPPI-T100, and OCHPPI-T150 after the friction test was characterized by SEM and a noncontact surface profiler. To meet the needs of morphology testing, the rubbed samples were washed with petroleum ether as a solvent in a Soxhlet extractor to remove the lubricant stored in matrix. Figure 7 displays the surface morphology of the rubbed samples. The results show that the large pores on the surface of HPPI-T50, HPPI-T100, and HPPI-T150 were not blocked or collapsed. Only the micropillars of HPPI-T150 underwent a certain degree of plastic deformation, while the micropillars of HPPI-T100 underwent slight plastic deformation. In addition, plastic deformation was investigated from the small pores, which caused the small pores to be partially blocked. Figure 8 shows the three-dimensional morphology and wear rate. The width of the wear scar can be compared in the following sequence: OCHPPI-T100 < OCHPPI-T150 < OCHPPI-T50 < OCPPI. The result of wear rate in Fig. 8(e) shows that OCHPPI-T100 is the smallest among all rubbed samples, and OCPPI is the largest. OCHPPI, especially OCHPPI-100, exhibits excellent tribological performance.

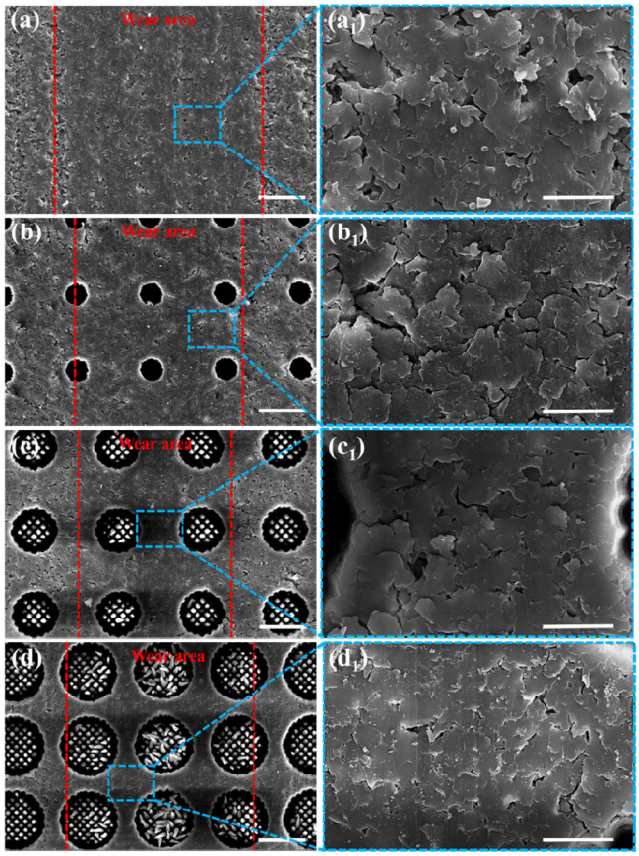

Fig. 7 Surface morphology of (a) PPI, (b) HPPI-T50, (c) HPPI-T100, and (d) HPPI-T150 after the friction experiment (the scale bar in the left image is 100 μm, and right is 30 μm).

The friction and wear of porous oil-containing material mainly arise from the solid–solid contact between the counterpart and the porous matrix, and the lubricating film between the interface is the main reason for reducing friction and wear [26]. The different thicknesses of the lubricating film might be the reason why the samples had different tribological performances. For OCPPI, the higher friction and

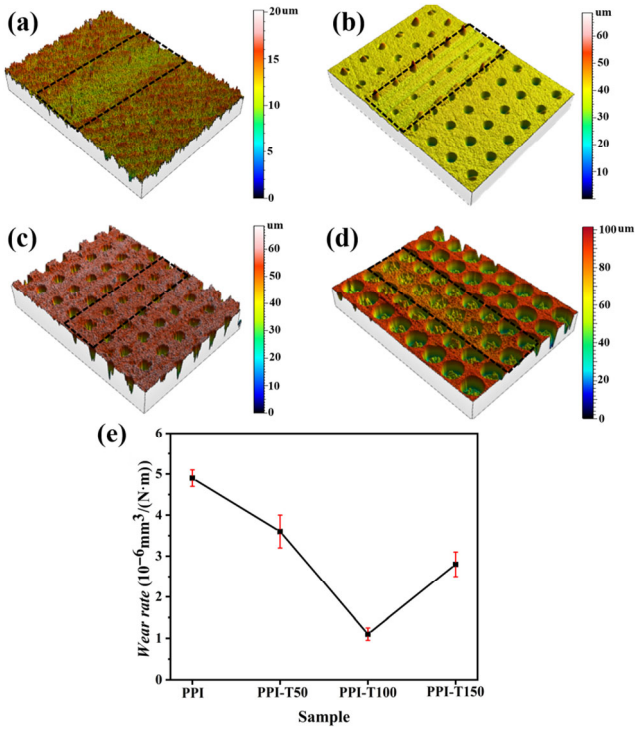

Fig. 8 Surface morphology of (a) OCPPI, (b) OCHPPI-T50, (c) OCHPPI-T100, and (d) OCHPPI-T150 after the friction experiment and (e) wear rate of rubbed samples.

wear might be ascribed to less oil release, resulting in the samples being in boundary lubrication state. At the same time, the surface asperity caused solid-solid contact between the matrix and counterpart, which caused partial blockage of the surface pore structure and further increased the wear, as the lubricant could not continuously and stably release. However, for OCHPPI-T50, OCHPPI-T100, and OCHPPI-T150, although the small pores on the surface were inevitably blocked during the friction process, the PAO10 stored in the large pores could still release to the interface and form a thicker oil film. The thicker oil film reduced the direct solid-solid contact between the counterpart and the porous matrix. In addition, the internal micropillars (Figs. 7(c) and 7(d)) underwent different degrees of plastic deformation. The plastic deformation of micropillars exhibited that the contact area between the counterpart and the porous matrix was smaller than that of the large pores, which caused more lubricant to be squeezed out and a much thicker oil film to form on the interface [27]. Nonetheless, although the large pores of HPPI-T150 can store more lubricant, the friction and wear did not decrease further with the increase in the large pore size. The roughness of the HPPI-T150 was larger than that of PPI due to the introduction of large pores, so a larger shear force (a type of mechanical force) was generated during the friction process. Furthermore, the small gap between the large pores (only 50 μm) caused stress concentration and solid-solid contact [33]. For HPPI-T50, the large pores could store a small amount of lubricating oil, and less lubricant was released to the surface. Although the roughness generated by large pores was less than that of OCHPPI-T100 and OCHPPI-T150, the friction and wear were more obvious due to the thinner oil film thickness and thus the more serious solid-solid contact. For OCHPPI-T100, the large pores (pore size = 100 μm) did not cause obvious stress concentration (the gap between the large pores was 100 μm), released more lubricant and formed a thicker oil film. Therefore, OCHPPI-T100 exhibited excellent tribological performance.

As mentioned above, the amount of oil release is an important factor affecting the difference in lubrication performance of OCHPPI-T50, OCHPPI-T100, and OCHPPI-T150. Stimulus-responsive oil release of oil-containing samples was characterized by weighing the mass before and after stimulation. Filter paper was selected to absorb the released lubricant, which prevented the released lubricant from sucking back into the porous substrate. The oil-containing sample was placed in an oven at 50 °C to simulate the frictional heat stimulus, and 50 N weights were loaded on the oil-containing samples to simulate the mechano-stimulus during the friction process.

The result of stimulus-responsive oil release is shown in Fig. 9, which indicates that the amount of oil released under the thermal-and-mechano-stimuli increases significantly as the large pore size increases. The differential volume expansion (the thermal expansion coefficient of PAO10 is 7.6×10^{-4} °C^{-1}, and that of polyimide matrix is 4.2×10^{-5} °C^{-1}) between the porous matrix and the PAO 10 realized the lubricant release. Simultaneously, the slight deformation of porous matrix under mechano-stimulus realized the lubricant release. The lubricant impregnated in HPPI could release more lubricant in response to thermal-and-mechano-stimuli, which further affected the lubrication performance.

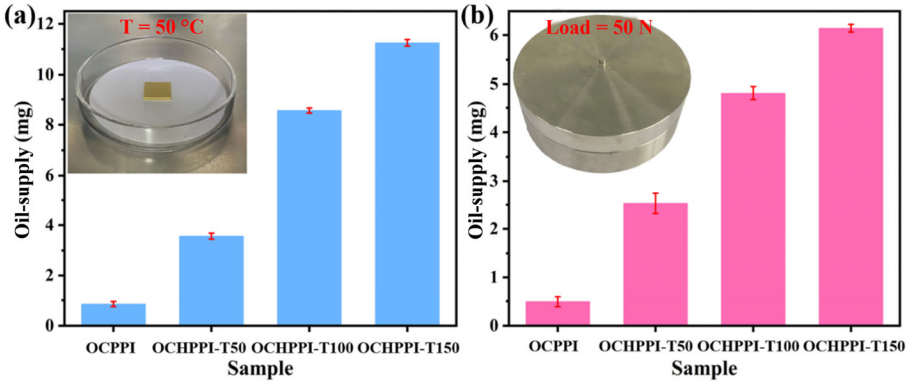

Fig. 9 Oil supply of different samples under (a) thermal-stimulus and (b) mechano-stimulus.

In addition, the influence of the large pores and the small pores on the tribological performance was studied. To study the effect of large pores on the lubrication performance, OCHPPI-T100 and OCPPI were applied for friction tests under 10 N and variable frequency of 1–20 Hz, and the test lasted 150 min. The COF evolution of OCPPI and OCHPPI-T100 in Fig. 10 exhibits a behavior that closely resembles that of a Stribeck curve. However, the COF values of OCHPPI-T100 are less than that of OCPPI in the whole friction test process. At a frequency of 1 Hz, the COF of OCPPI is approximately 0.12, while that of OCHPPI-T100 is approximately 0.07. At a speed of 13 Hz, the COF values of OCHPPI-100 and OCPPI are the lowest (the COF of OCHPPI-T100 is 0.024 and that of OCPPI is 0.051).

In the case of OCHPPI-T100, however, 1) the large pores on the surface could store more oil and release oil spontaneously; 2) the higher oil-content produced by large pores resulted in releasing more oil to the interface and better lubrication conditions, which could form thicker oil film and reduce the shear forces, hence mitigating friction and wear.

Additionally, the tribological properties of OCPI-T100 and OCHPPI-T100 were tested under the same working conditions as in Section 3.2 to investigate the effect of small pores on the lubrication performance. The result is shown in Fig. 11. In the first 90 min, the COF of OCPI-T100 decreases from 0.09 to 0.08. From 90 to 120 min, the COF only decreases by 0.02 (the COF is 0.06), which is much larger than the COF of OCHPPI-T100 (COF = 0.024) at this frequency, and finally increases to 0.08.

Although OCPI-T100 can release the lubricant from large pores, the lubricant released from the large pores was squeezed out on the gap between the large pores and only formed a molecular-thin oil film. However, for OCHPPI-T100, there were many small pores in the gap between the large pores, which can directly supply lubricant to the interface. The synergistic effect of large pores and small pores of OCHPPI-T100

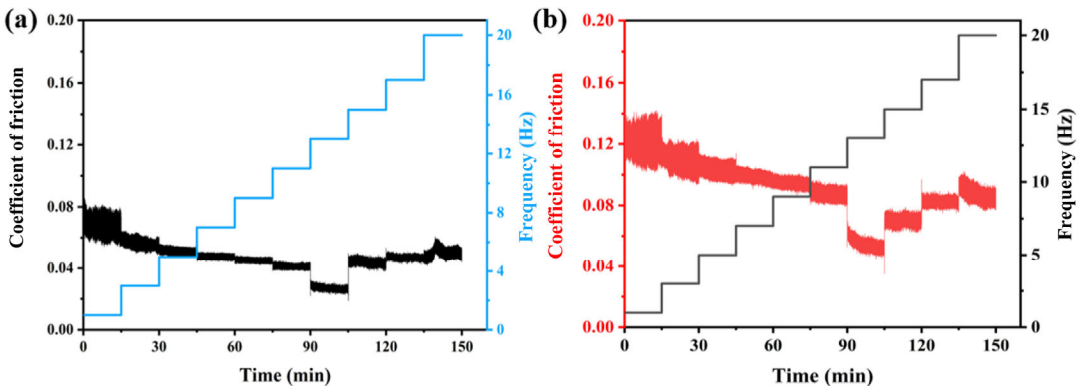

Fig. 10 Evolution of COF with time during a frequency ramp test from 1 to 20 Hz (load = 10 N, and the frictional test lasted 150 min) for (a) OCHPPI-T100 and (b) OCPPI.

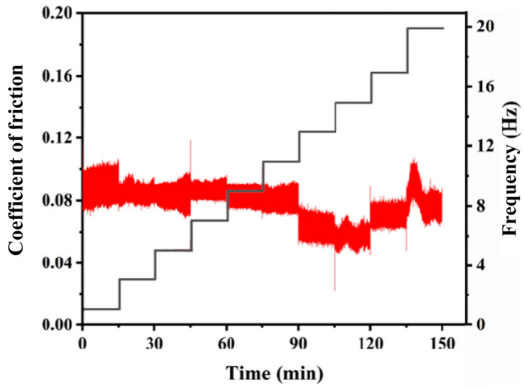

Fig. 11 Evolution of COF with time during a frequency ramp test from 1 to 20 Hz (load = 10 N, and the frictional test lasted 150 min) for OCPI-T100.

was able to continuously release oil to the interface and significantly reduced the friction and wear.

3.3 Stimuli-response and recycling smart lubrication performance of hierarchical pore structure

The aforementioned results show that OCPPI, OCHPPI-T50, OCHPPI-T100, and OCHPPI-T150 can release oil to the interface under thermal-and-mechano-stimulus. To study smart lubrication with recyclable oil release/reabsorption performance, the oil release of OCHPPI-T100 and OCPI-T100 and capillary-force induced oil reabsorption were characterized. Figures 12 and 13 show red oil spot (PAO10 stained with red dye.) on filter paper, which indicates that the lubricant stored in OCHPPI-T100 and OCPI-T100 could be released under thermal-and-mechano-stimuli. To investigate the lubricant absorption performance, the oil-proof paper was selected. The results in Fig. 12 show that no obvious red oil spot is observed on the oil-proof paper, indicating that the lubricant was absorbed into the matrix by the capillary-forces when the thermal-and-mechano-stimuli were removed. However, the results in Fig. 13 show that obvious red oil spots are observed on the oil-proof paper, which demonstrates that only part of the lubricant was absorbed into the matrix by the capillary-forces when the thermal-and-

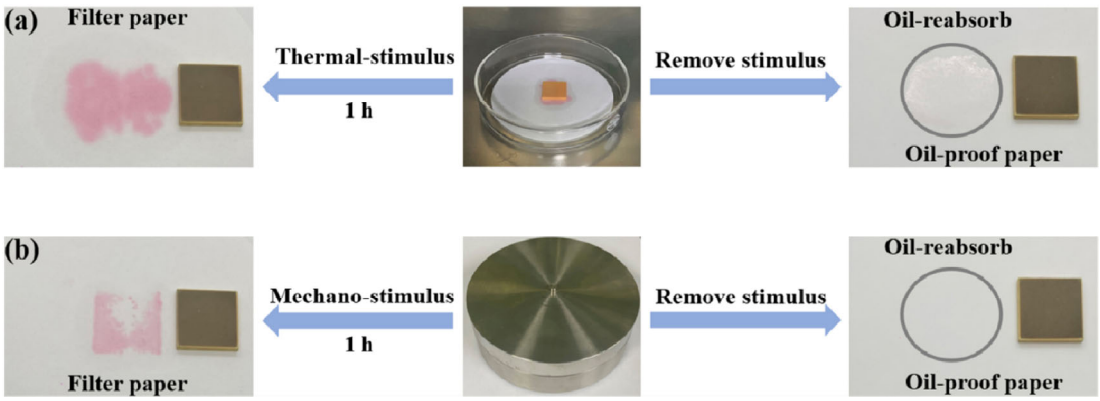

Fig. 12 Oil release of OCHPPI-T100 under (a) thermal-stimulus or (b) mechano-stimulus and capillary force induced oil reabsorption.

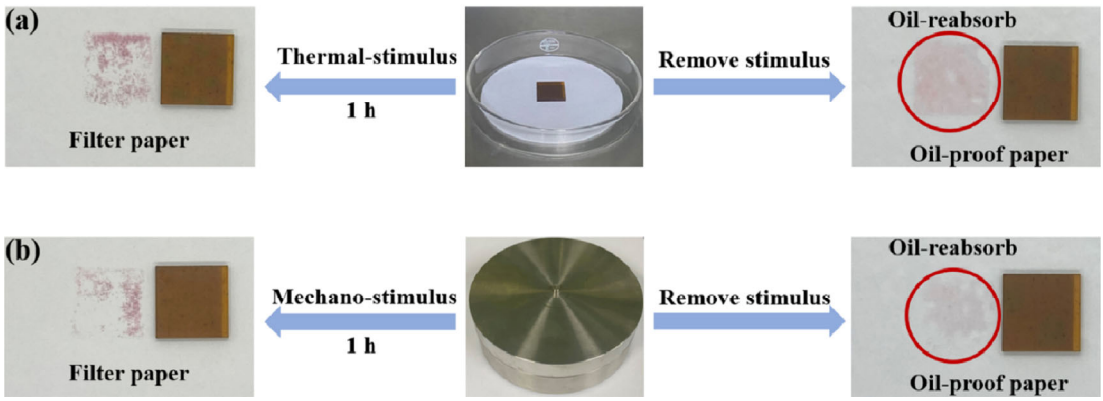

Fig. 13 Oil release of OCPI-T100 under (a) thermal-stimulus or (b) mechano-stimulus and capillary-force induced oil reabsorption.

mechano-stimuli were removed. By weighing the oil-proof paper before and after the test, for OCPI-T100, it was found that the lubricant remaining on oil-proof paper was 1.42 mg after removing the thermal-stimulus and 0.63 mg after removing mechano-stimulus. For OCHPPI-T100, the lubricant remaining on oil-proof paper was 0.21 mg after removing the thermal-stimulus and 0.12 mg after removing mechano-stimulus. The small pores in HPPI facilitated the oil reabsorption. The schematic diagram of thermal-and-mechano-stimuli response recyclable lubricant release/reabsorption of hierarchically porous oil-containing polyimide is shown in Fig. 14.

Longevity is important for lubrication materials. To investigate the life of OCHPPI-T100, the same position of OCHPPI-T100 was conducted 30 cycles during the friction test, and each test lasted 1 h. A load of 10 N and a frequency of 5 Hz were applied for the friction test. To avoid the effect of oil film formed on counterpart on the tribology test, replacing with a new steel ball after each test. As a control, OCPPI was tested 30 cycles under the same conditions as OCHPPI-T100. Both OCPPI and OCHPPI-T100

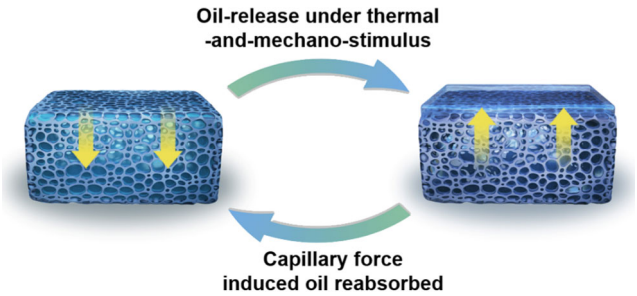

Fig. 14 Schematic diagram of recyclable lubricant release/reabsorption of hierarchically porous oil-containing polyimide.

(Fig. 15(a)) maintain a stable COF under 30 cycles friction experiment, and the COF of OCHPPI-T100 is lower than that of OCPPI, which was ascribed to the more lubricant released.

It is challenging to perform thousands of recycled lubrication tests on the same sample. As aforementioned, the oil released to the interface determined the friction and wear performance. Therefore, the maximum lubricant released was tested. Because lubricant release of the hierarchically porous oil-containing material was a synergetic effect of the thermal-and-mechano-stimuli, 40 °C and 100 N were selected to test the maximum oil release. Additionally, the oil loss during each recyclable smart lubrication process was unavoidable, such as transfer to the counterpart. From Section 3.2, it can be found that OCHPPI-T100 experienced plastic deformation after the friction test, but no damage or wear debris was generated. Therefore, the weight change of OCHPPI-T100 before and after the friction test was ascribed to the loss of lubricant (transferred to counterpart or leakage). Therefore, the life of OCHPPI-T100 and OCPPI can be achieved from the maximum amount of oil released divided by the amount of oil consumed in each friction test. The OCPPI and OCHPPI-T100 were placed in an oven at 40 °C, and a load of 100 N was applied for different durations to simulate the thermal-and-mechano-stimuli of the friction and measure the maximum oil release. The released oil was wiped off every 2 h within 12 h, and the mass of hierarchically porous oil-containing polyimide was recorded (Fig. 15(b)). The oil release decreased with the increase of thermal-and-mechano-stimuli period until the maximum oil release was obtained at 12 h,

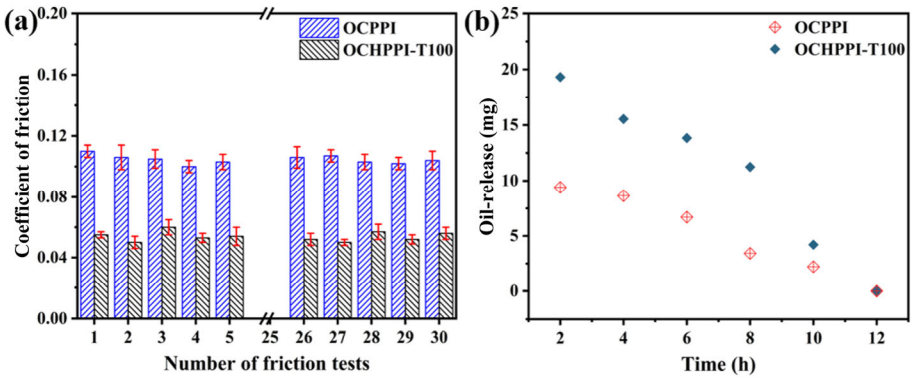

Fig. 15 (a) COF from the first to the 30th time (load = 10 N, frequency = 5 Hz, and the frictional test lasted 60 min) for OCPPI-T100 and OCPPI and (b) the maximum oil release for OCPPI-T100 and OCPPI.

and the maximum oil release of OCHPPI-T100 was 64.16 mg and that of OCPPI was 30.41 mg. The lubricant loss of OCPPI and OCHPPI-T100 after per cycle smart lubrication was approximately 0.05 and 0.06 mg, respectively. Hence, OCPPI and OCHPPI-T100 can perform 608 and 1,069 recyclable smart lubrication experiments with a duration of 1 h each time. Compared with OCPPI, the life of OCHPPI-T100 was increased by 75.8%. The hierarchical pore structure can significantly extend the life of porous oil-containing recyclable smart lubrication materials.

4 Conclusions

A new hierarchically porous oil-containing material with higher oil-content, excellent tribological properties, and smart-lubrication was successfully fabricated.

1) Porous polyimide (PPI) with a hierarchical pore structure not only had a high oil-content but also maintained the mechanical strength and oil-retention.

2) The excellent lubrication performance of hierarchically porous oil-containing polyimide was ascribed to storing more lubricant, and then the oil-containing sample could release more lubricant to the interface under the thermal-and-mechano-stimuli and form a thicker lubricating oil film to reduce the solid-solid contact between the counterpart and porous matrix.

3) The stimulus-response oil release and capillary-force induced oil reabsorption of hierarchically porous oil-containing polyimide laid a solid foundation for recyclable smart lubrication performance. The smart lubrication process of OCHPPI-T100 could be realized 1,069 times (each time lasted 1 h), which significantly extended the life of the hierarchically porous oil-containing lubrication material.

Acknowledgements

This research was financially supported by the National Key R&D Program of China (2020YFB2006901), National Natural Science Foundation of China (51935006), CAS Project for Young Scientists in Basic Research (YSBR-023), Youth Innovation Promotion Association of Chinese Academy of Sciences (Grant No. 2020417), and Key Research Program of the Chinese Academy of Sciences (XDPB24).

Open Access This article is licensed under a Creative Commons Attribution 4.0 International License, which permits use, sharing, adaptation, distribution and reproduction in any medium or format, as long as you give appropriate credit to the original author(s) and the source, provide a link to the Creative Commons licence, and indicate if changes were made.

The images or other third party material in this article are included in the article's Creative Commons licence, unless indicated otherwise in a credit line to the material. If material is not included in the article's Creative Commons licence and your intended use is not permitted by statutory regulation or exceeds the permitted use, you will need to obtain permission directly from the copyright holder.

To view a copy of this licence, visit http://creativecommons.org/licenses/by/4.0/.

References

[1] Ruan H, Shao M, Zhang Y, Wang Q, Wang C, Wang T. Supramolecular oleogel-impregnated macroporous polyimide for high capacity of oil storage and recyclable smart lubrication. *ACS Appl Mater Interfaces* **14**(8): 10936–10946 (2022)

[2] Yu Q, Fan M, Li D, Song Z, Cai M, Zhou F, Liu W. Thermoreversible gel lubricants through universal supramolecular assembly of a nonionic surfactant in a variety of base lubricating liquids. *ACS Appl Mater Interfaces* **6**(18): 15783–15794 (2014)

[3] Kerni L, Raina A, Irfan MIU. Friction and wear performance of olive oil containing nanoparticles in boundary and mixed lubrication regimes. *Wear* **426–427**: 819–827 (2019)

[4] Tang J, Chen S, Jia Y, Ma Y, Xie H, Quan X, Ding Q. Carbon dots as an additive for improving performance in water-based lubricants for amorphous carbon (aC) coatings. *Carbon* **156**: 272–281 (2020)

[5] Kumari S, Chouhan A, Sharma P, Tawfik A, Tran K, Spencer J, Bhargava K, Walia S, Ray A, Khatri P. Surface functionalization of WS_2 nanosheets with alkyl chains for enhancement of dispersion stability and tribological properties. *ACS Appl Mater Interfaces* **14**(1): 1334–1346 (2021)

[6] Singh N, Sinha K. Tribological performances of hybrid composites of Epoxy, UHMWPE and MoS_2 with in situ liquid lubrication against steel and itself. *Wear* **486**: 204072 (2021)

[7] Vyavhare K, Timmons B, Erdemi A, Edwards L, Aswath B. Robust interfacial tribofilms by borate-and polymer-coated ZnO nanoparticles leading to improved wear protection

under a boundary lubrication regime. *Langmuir* **37**(5): 1743–1759 (2021)

[8] Dong F, Hou G, Cao F, Yan F, Liu L, Wang J. The lubricity and reinforcement of carbon fibers in polyimide at high temperatures. *Tribol Int* **101**: 291–300 (2016)

[9] Li S, Duan C J, Li X, Shao M C, Qu C H, Zhang D, Wang Q H, Wang T M, Zhang X R. The effect of different layered materials on the tribological properties of PTFE composites. *Friction* **8**(3): 542–552 (2020)

[10] Duan C, Yuan D, Yang Z, Li S, Tao L, Wang Q, Wang T. High wear-resistant performance of thermosetting polyimide reinforced by graphitic carbon nitride (g-C_3N_4) under high temperature. *Compos Part A: Appl Sci Manufac* **113**: 200–208 (2018)

[11] Ragupathi K, Mani I. Durability and lube oil contamination study on diesel engine fueled with various alternative fuels: A review. *Energy Sources, Part A* **43**(8): 932–943 (2018)

[12] Gong H, Yu C, Zhang L, Xie G, Guo D, Luo J. Intelligent lubricating materials: A review. *Compos Part B: Eng* **202**: 108450 (2020)

[13] Zhang G, Xie G, Si L, Wen S, Guo D. Ultralow friction self-lubricating nanocomposites with mesoporous metal–organic frameworks as smart nanocontainers for lubricants. *ACS Appl Mater Interfaces* **9**(43): 38146–38152 (2017)

[14] Shao M, Li S, Duan C, Yang Z, Qu C, Zhang Y, Zhang D, Wang C, Wang T, Wang Q. Cobweb-like structural stimuli-responsive composite with oil warehouse and transportation system for oil storage and recyclable smart-lubrication. *ACS Appl Mater Interfaces* **10**(48): 41699–41706 (2018)

[15] Ruan H, Zhang Y, Li S, Yang L, Wang C, Wang T, Wang Q. Effect of temperature on the friction and wear performance of porous oil-containing polyimide. *Tribol Int* **157**:106891 (2021)

[16] Wang C, Zhang D, Wang Q, Ruan H, Wang T. Effect of porosity on the friction properties of porous polyimide impregnated with poly-α-olefin in different lubrication regimes. *Tribol Lett* **68**(4): 1–9 (2020)

[17] Ji Z, Xie G, Xu W, Wu S, Zhang L, Luo J. Self-cleaning of interfacial oil between polymer composites with porous zeolite microparticles and their self-lubrication properties. *Adv Mater Interfaces* **6**(10): 1801889 (2019)

[18] Gheisari R, Lan P, Polycarpou A. Efficacy of surface microtexturing in enhancing the tribological performance of polymeric surfaces under starved lubricated conditions. *Wear* **444–445**: 203162 (2020)

[19] Rosenkranz A, Costa L, Baykara Z, Martini A. Synergetic effects of surface texturing and solid lubricants to tailor friction and wear – A review. *Tribol Int* **155**: 106792 (2021)

[20] Ruan H, Zhang Y, Wang Q, Wang C, Wang T. A novel earthworm-inspired smart lubrication material with self-healing function. *Tribol Int* **165**: 107303 (2022)

[21] Zhang D, Wang C, Wang Q, Wang T. High thermal stability and wear resistance of porous thermosetting heterocyclic polyimide impregnated with silicone oil. *Tribol Int* **140**: 105728 (2019)

[22] Marchetti M, Meurisse M, Vergne P, Sicre J, Durand M. Analysis of oil supply phenomena by sintered porous reservoirs. *Tribol Lett* **10**(3): 163–170 (2001)

[23] Wang J, Zhao H, Huang W, Wang X. Investigation of porous polyimide lubricant retainers to improve the performance of rolling bearings under conditions of starved lubrication. *Wear* **380**: 52–58 (2017)

[24] Zhu Y, Wang G, Wang H, Zhang S, Yang S. Tribological properties of porous PPS/PTFE composite filled with mesopore titanium oxide whisker. *J Appl Polym Sci* **129**(4): 2321–2327 (2013)

[25] Wang H, Li M, Liu D, Zhao Y, Zhu Y. Tribological properties tests and simulations of the nano-micro multilevel porous self-lubricating PEEK composites with ionic liquid lubrication. *J Mater Sci* **51**(8): 3917–3927 (2016)

[26] Wang H, Wang G, Zhang S, Yang S, Zhu Y. Tribological performances on porous polyphenylene sulfide self-lubricating composites with super wear resistance. *J Thermoplast Compos Mater* **27**(1): 82–92 (2014)

[27] Yang X, Chen L, Li Y, Rooke C, Sanchez C, Su B. Hierarchically porous materials: synthesis strategies and structure design. *Chem Soc Rev* **46**(2): 481–558 (2017)

[28] Ding Y, Huang L, Barakat T, Su B. A novel 3DOM TiO_2 based multifunctional photocatalytic and catalytic platform for energy regeneration and pollutants degradation. *Adv Mater Interfaces* **8**(4): 2001879 (2021)

[29] Sun M, Huang S, Chen L, Li Y, Yang X, Yuan Z, Su B. Applications of hierarchically structured porous materials from energy storage and conversion, catalysis, photocatalysis, adsorption, separation, and sensing to biomedicine. *Chem Soc Rev* **45**(12): 3479–3563 (2016)

[30] Dorin M, Sai H, Wiesner U. Hierarchically porous materials from block copolymers. *Chem Mater* **26**(1): 339–347 (2014)

[31] Zhang D, Wang T, Wang Q, Wang C. Selectively enhanced oil retention of porous polyimide bearing materials by direct chemical modification. *J Appl Polym Sci* **134**(29): 45106 (2017)

[32] Kaufmann J, Loser R, Leemann A. Analysis of cement-bonded materials by multi-cycle mercury intrusion and nitrogen sorption. *J Colloid Interface Sci* **336**(2): 730–737 (2009)

[23] Su B, Huang L, Huang W, Wang X. The load carrying capacity of textured sliding bearings with elastic deformation. *Tribol Int* **109**: 86–96 (2017)

Tingmei WANG. She is currently a researcher and doctoral supervisor at Lanzhou Institute of Chemical Physics, Chinese Academy of Sciences, China. She received her bachelor degree (1992) in Department of Organic Chemical Engineering, Northwest University and Ph.D. degree (2003) in Lanzhou Institute of Chemical Physics, Chinese Academy of Sciences. Her current research interests focus on design and preparation of porous polymer composites, design and development of polymer composites, preparation and properties of organic/inorganic nanocomposites, and development of high strength fiber reinforced composites. She has published over 200 journal papers and gained a number of awards.

Chao WANG. He is currently a researcher and doctoral supervisor at Lanzhou Institute of Chemical Physics, Chinese Academy of Sciences, China. He received his Ph.D. degree in Lanzhou Institute of Chemical Physics, Chinese Academy of Sciences. His current research interests focus on design and preparation of porous polymer composites, and design and development of smart lubrication material and polymer self-lubricating composites. He is a candidate for the talent project of "Light of West China" Program of Chinese Academy of Sciences, and Youth Innovation Promotion Association of Chinese Academy of Sciences.

Hongwei RUAN. He is a Ph.D. candidate in the Lanzhou Institute of Chemical Physics, Chinese Academy of Sciences, University of Chinese Academy of Sciences. His research focuses on the porous oil-containing material and the development of smart lubrication material.